VERTICAL DISTRIBUTION OF WIND SPEED, TEMPERATURE AND HUMIDITY ABOVE A WATER SURFACE[1]

By

R. G. FLEAGLE J. W. DEARDORFF F. I. BADGLEY

University of Washington

ABSTRACT

An observational program is described which has been used to obtain an accurate determination of vertical profiles of wind speed, temperature, and vapor pressure over a salt water inlet with an over-water air fetch of about five miles. The wind profiles show systematic anomalies of 1 or 2 ‰, which are not explainable as instrumental or observational error. The curvature of wind profiles over water shows the same dependence on Richardson number as that found by others over land. Temperature profiles are similar in this respect, but curvature of the vapor pressure profiles shows little dependence on stability. Values of the resistance coefficient computed from wind profiles are at the lower limit of those reported by most other investigators. Analogous coefficients computed from temperature and vapor pressure profiles have the same magnitude as the resistance coefficient but show a greater dependence on stability.

INTRODUCTION

One would like to specify the energy and mass transfer at the earth's surface in terms of as simple a set of atmospheric parameters as possible. At its simplest, this set might be wind speed, temperature and humidity at the surface and at a single height above; more realistically it might be vertical distributions of wind speed, temperature and humidity in the air near the surface. However, if one attempts to achieve the latter for the great ocean areas, he finds that there are few data available from which transfer calculations can be made; and worse, observations vary to such an extent that, for example, the roughness lengths reported from various studies under apparently similar conditions differ by several orders of magnitude. This represents an unexplained difference in drag coefficient of an order of magnitude which is obviously intolerable if one

[1] Contribution No. 48, Department of Meteorology and Climatology, University of Washington. Publication was supported in part by The Agnes H. Anderson Fund of The University of Washington.

wants to understand wind stress on the water. These considerations illustrate the need for reliable observations over the oceans.

An observational program conducted during the past few summers at the Friday Harbor Laboratories of the University of Washington has been designed to meet part of this need.

FIELD EQUIPMENT AND METHOD OF OBSERVATION

Wind speeds at eight levels, from 31 to 442 cm above the water surface, were measured with sensitive rotating cup anemometers manufactured by Casella after Sheppard's design. These were supported above the water by an anchored skeleton raft 20 feet square, with buoyant tanks located at its four corners. These tanks barely supported the weight and therefore responded only slowly to passing waves (see Fig. 1). A horizontal plywood disk was mounted eight feet below each of the four tanks to further reduce rocking due to waves. In all waves encountered, vertical motion or rocking of this raft was unnoticeable.

The anemometers were supported from a central mast ($^3/_4$ inch galvanized iron pipe) from which individual supports extended two feet horizontally outward. As shown in Fig. 1, the lower six were arranged alternately on either side of the mast and were pointed slightly upwind to eliminate interference between adjacent anemometers and between mast and anemometers. The top two instruments had enough vertical spacing so that their supports could be pointed directly into the wind. Seven of these anemometers, of the electrical contact type, were connected by underwater cable to counters on an anchored log raft shown at the left of Fig. 1; one anemometer with dial was read with the aid of field glasses from that raft. The anemometers were carefully compared in a variety of wind conditions prior to observation and corrected calibration curves were constructed. The authors are confident that the hourly response of each anemometer was known to within about 2 cm/sec of the response of the anemometer that was used as standard. Four of the anemometers were compared at low wind speeds after the observations were completed and no change in calibration was noted.

Dry and wet-bulb temperatures were determined at 40, 80, 160 and 320 cm above the surface by a micropsychrometer made of two 40 gauge copper-constantan thermocouples. This instrument was mounted on a vertical wire track which ran upward from the water surface three feet outboard from the raft shown at the far left of Fig. 1. The micropsychrometer was raised and lowered manually through the desired vertical range and was ventilated by natural wind. A thermos bottle of sea water, collected at the surface at 15 minute intervals, served as the reference temperature; the thermo-

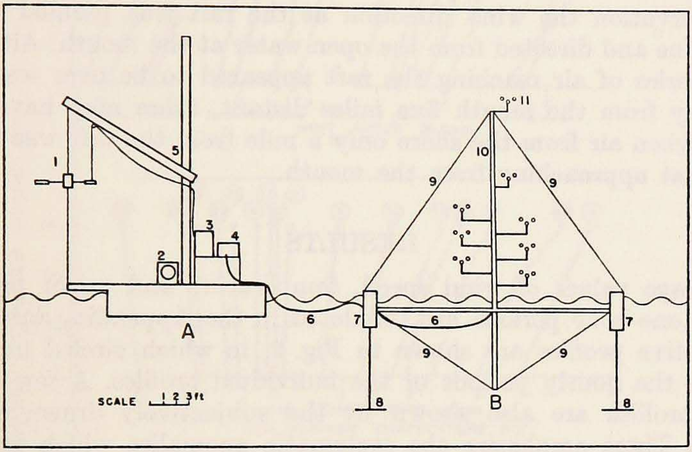

Figure 1. Sketch showing recording raft (A) and anemometer raft (B) viewed from upwind. Shown are: Thermocouple psychrometer (1), generator (2), D.C. amplifier and thermocouple outputs (3), wind register (4), mast and yard-arm (5), underwater cable (6), floats (7), wave dampers (8), guy wires (9), anemometer mast (10), anemometer (11).

couple output was read visually from a Leeds and Northrup Model 9835 B D.C. amplifier. A series of readings was made each minute; these consisted of two readings of temperature and one of wet-bulb temperature at each level. Thus average time between readings was five seconds, an interval which was considered to be sufficiently long to absorb the lags of thermocouples and amplifier and to allow the observer to make accurate readings representative of about one second.

Made at the same time but not reported in this paper were observations of solar and infra-red radiation, of evaporation from a floating pan, and of diffusion of particulate matter; the latter observations were made by a group from the Hanford Laboratories of The General Electric Company.

Observations were made during a four-day period in July 1958 in the center of East Sound, a salt water inlet about one mile wide, seven miles long, and 90 feet deep. East Sound opens to the south and is surrounded on the other three sides by Orcas Island, located in the San Juan Archipelago between Vancouver Island and the mainland at about Lat. 49° N. The shores on both sides of East Sound rise rather abruptly to a height of several hundred feet, but the terrain at the closed north end is low and flat. During the period of observation the wind direction at the raft was parallel to the shore line and directed from the open water at the mouth. Although trajectories of air reaching the raft appeared to be over water all the way from the mouth five miles distant, there may have been times when air from the shore only a mile from the raft was mixed into that approaching from the mouth.

RESULTS

Average values of wind speed, temperature and vapor pressure for 30 one-hour periods are tabulated in the Appendix. Some representative profiles are shown in Fig. 2, in which circled numbers specify the hourly periods of the individual profiles. A few of the wind profiles are also shown by the subjectively drawn dashed curves. These emphasize the systematic anomalies which are 1 or 2 $^0/_0$ of the wind speed. No such anomalies are evident in the temperature and vapor pressure profiles. Individual measurements of these profiles relative to the reference values are considered to have maximum errors, due to sampling, of .02° C and .04 mb, respectively. There probably is a greater uncertainty in the sea surface temperature than in the above because it was sampled only four times during each hour; also there is a corresponding ambiguity in the wind speed relative to the sea surface because surface drift has been neglected.

Details of Wind Profiles. Many investigators have found that wind profiles are smooth curves when based on measurements made over uniform land surfaces. Under conditions of neutral hydrostatic stability, the curves become straight lines if the wind speed is plotted against the logarithm of the height, z. In stable air such plotted curves are slightly convex towards the log z axis, and in unstable air the curvature is reversed (Deacon, 1949). While the velocity profiles shown in Fig. 2 are in general agreement with the above, the readings from anemometers at 60, 133, and 213 cm, which are those shown on the left of the mast in Fig. 1, are with

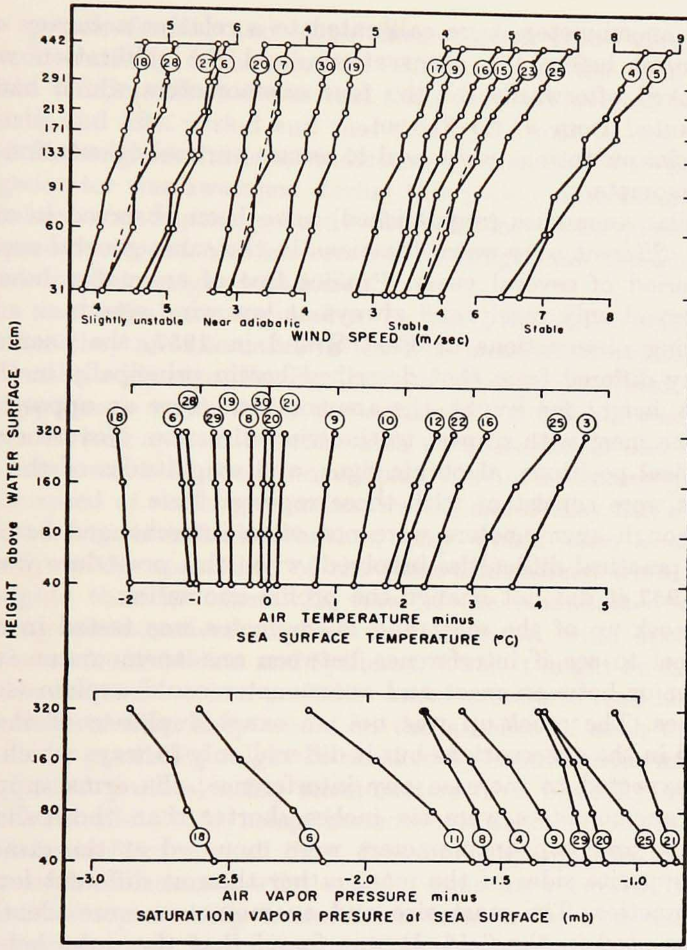

Figure 2. Representative profiles of wind, temperature, and vapor pressure.

two exceptions higher than would be predicted from smooth curves drawn for the other levels. This throws suspicion on the calibration and installation of the instruments; in particular, since the anemometers giving anomalously high readings were on the opposite side of the mast from the others, it seems possible that the rotation of the anemometer cups was influenced by the presence of the mast or of the other anemometers. In recognition of these possibilities the following considerations are pertinent:

1) The anemometers were calibrated to a relative accuracy of 1 or 2 cm/sec before the observations, and the calibration was rechecked afterwards for the four anemometers which had been mounted from 91 to 213 cm.
2) Special mountings were used to assure vertical orientation of the anemometers.
3) Similar anomalies (unpublished) have been observed in at least five different over-water locations in the same general area over a period of several years. Profiles free of anomalies have been observed only rarely and always at low wind speeds.
4) During observations at East Sound in 1957, the anemometer array differed from that described herein principally in the fact that, height for height, the anemometers were on opposite sides of the mast with respect to the wind direction. Nevertheless the vertical positions, algebraic signs, and magnitudes of the anomalies were consistent with those reported here.
5) Although anemometers were not often interchanged because of the practical difficulties involved, when this procedure was tried in 1957 it did not change the profile anomalies.
6) A mock-up of the mast and anemometer was tested in a wind tunnel to see if interference between one anemometer and another or between mast and anemometer could explain the anomalies. The mock-up was not an exact duplicate of the mast used in the observations but it differed only in ways which would be expected to increase any interference: the arms supporting the anemometers were six inches shorter than those shown in Fig. 1, and two anemometers were mounted at the same level on opposite sides of the mast rather than at different levels, as in practice. The mast size and anemometers were identical to those used in the field. It was found that the wake behind an obstacle, whether anemometer or mast, affected the reading of a second anemometer only if the latter were within 30° of being directly downstream of the obstacle. This extreme was never the case in practice.

In view of the above it is difficult to accept an explanation based on a presumption of persistent errors in calibration or mounting of the instruments, but further investigation of this point is called for.

A final bit of evidence suggests that what has been observed here is an effect of waves at the surface. Throughout periods 1 through

4, the second, fourth, and sixth anemometers from the bottom indicated relatively high velocities compared to the first, third, and fifth. Wind profile 5 shows that these features reversed between the fourth and fifth period and that during the fifth period the sea reached its roughest state, as indicated by the fact that the electrical generator was swamped during this period, thus interrupting temperature and vapour pressure observations. Subsequently, the wind speed decreased, the sea became less rough, and the anomalies returned to their original positions.

If the anomalies are presumed to be 'real', it is still uncertain as to whether they are anomalies in the true mean wind velocity profile or in the eddy size distribution. An explanation based on the latter hypothesis would infer the existence of ordered vortices in the form of long cylindrical rolls with axes horizontal and normal to the mean wind. If these moved past the anemometers (perhaps with the speed of the larger surface waves) and if they had a persistent size and vertical distribution, they would then contribute differently to the variability of the three-dimensional wind at certain heights than at others. In view of the complicated way in which cup anemometers respond to changes in wind speed and angle of attack (Middleton and Spilhaus, 1953), it might be expected that these ordered vortices prejudice anemometers to read higher at certain heights than they would in the absence of such vortices.

The above possibility might be checked by simultaneous measurement of wind profiles, using anemometers of a basically different design. Takahashi (1958), using thermocouple anemometers mounted at five heights from a small boat, found an apparent discontinuity of slope of his measured wind speed versus log z curves. This he explained as representing a transition from a 'hydrodynamically rough' profile which had been established over land to a 'hydrodynamically smooth' profile becoming established over the water. This explanation is inadequate to account for the several kinks in the more detailed wind profiles of Fig. 2.

Effect of Thermal Stratification. The outstanding feature of the wind and temperature profiles shown in Fig. 2 is their logarithmic form in near-adiabatic conditions and a stability effect as previously mentioned. However this effect appears to be less consistent among the vapor pressure profiles.

The influence of stability upon wind profile has been expressed by Lettau (1949), Panofsky (1952), Monin and Obukhov (1953), Businger (1955), Sheppard (1958), and others by the 'log plus linear' equation as a first approximation. This equation arises if it is assumed that

$$K_m = k\sqrt{\tau/\varrho}\, z/(1 - mz), \tag{1}$$

where K_m is the eddy viscosity defined by

$$\tau/\varrho = K_m \frac{\partial u}{\partial z}. \tag{2}$$

Here u is the mean wind speed at height z; k, the Karman number; τ, the stress at the surface; ϱ, the density of the air; and m, a parameter existing in the presence of a turbulent vertical flux of enthalpy (heat). Upon substitution of (1) into (2) and on integration from surface to height z, the log plus linear equation is obtained:

$$u = (1/k)\sqrt{\tau/\varrho}\left(ln\frac{z+z_0}{z_0} - mz\right). \tag{3}$$

The common assumption has been made that the roughness length, z_0, appears in the numerator of the logarithmic term in order that u vanish at $z = 0$. Eq. (3) shows that the linear term produces a curvature to the logarithmic profile which has the expected sense when the sign of m is the same as the sign of the upward heat flux.

A dimensionless parameter which has frequently been used to describe the relative profile curvature is the Deacon number, β, defined by

$$\beta_q = -z\frac{\partial^2 q}{\partial z^2}\Big/\frac{\partial q}{\partial z}, \tag{4}$$

where q may represent wind speed, temperature, or the density of water vapor or other matter. From (1), (2), and (4), using $q = u$, it follows that $mz = (\beta_u - 1)/\beta_u$, so that (3) may be written

$$u = (1/k)\sqrt{\tau/\varrho}\left(ln\frac{z+z_0}{z_0} + \frac{1-\beta_u}{\beta_u}\right). \tag{5}$$

The Deacon number for wind, β_u, has been computed from (5), using winds at 31, 91, 171 and 442 cm. These levels were chosen so as to avoid levels at which the observed wind speed appeared to be systematically high for the reasons given previously. Values of β_u which then apply to a height of 161 cm are shown in Fig. 3 (crosses) plotted against the Richardson number, *Ri*, computed for the same height[2]. The *mz* scale for this height is given on the right-hand side

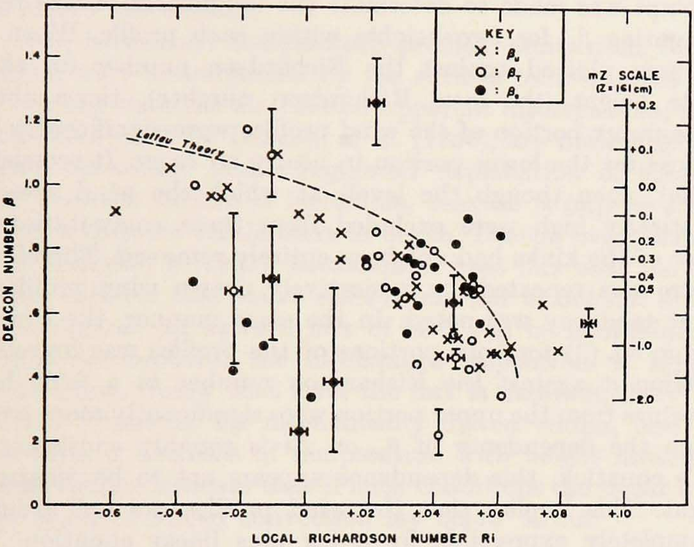

Figure 3. A plot *vs* local Richardson number, *Ri*, of Deacon's number, β (a measure of the relative profile curvature) for wind, temperature, and vapor pressure.

of Fig. 3. Assuming a standard deviation in relative wind speed measurements of ± 1 cm/sec, the standard error of β_u is approximately ±.04; for a standard deviation of temperature of ±.01° C, the standard deviation of *Ri* becomes about ±.002. The scatter of the β_u values appears to be somewhat larger than is to be expected from

[2] The Richardson number, usually thought of as a nondimensional measure of the stability of the atmosphere, is defined as:

$$Ri = g\left(\frac{\partial T}{\partial z} + \Gamma\right) \Big/ T\left(\frac{\partial u}{\partial z}\right)^2$$

where g is the acceleration of gravity, T, the Kelvin temperature, and Γ, the adiabatic lapse rate. In our computations Γ has been neglected because it is small compared to $\partial T/\partial z$ near the surface.

instrumental error alone, although plots of β_u against other stability parameters resulted in still greater scatter.

It has been shown by Lettau (1956) that β_u appears to be a unique function of Ri for over-land profiles, provided $Ri < .06$. His relation between β_u and Ri is shown by the curve in Fig. 3, which agrees fairly well with these over-water observations centered at 161 cm. An attempt was made to determine the uniqueness of this relation by computing β_u for two heights within each profile. When these values were plotted against the Richardson number for the appropriate height (the local Richardson number), those obtained from the upper portion of the wind profiles were significantly larger than those for the lower portion in nearly all cases. It seemed possible that, even though the levels at which the wind speed was systematically high were excluded from these computations, the influence of the kinks had not been entirely removed. Therefore the procedure was repeated for subjectively drawn wind profiles, but the same tendency was noted. In the same manner, the constancy of m from eq. (3) for both portions of the profiles was investigated by plotting it against the Richardson number at a fixed height. Again values from the upper portion were significantly more positive. Although the dependence of β_u on Ri is roughly consistent with Lettau's equation, this dependence appears not to be independent of height. This implies that the wind profiles are not accurately and completely expressible by a log plus linear equation. These negative conclusions are tentative, however, due to the uncertainty arising from the profile kinks.

The effect of stratification upon curvatures of temperature and moisture profiles may be investigated with the aid of the Deacon numbers for temperature and vapor pressure, β_T and β_e, respectively. These, computed from measurements at 40, 80, 160 and 320 cm, assuming log plus linear profiles, apply to a height of 112 cm. β_T is shown in Fig. 3 by open circles, β_e by solid circles. The line segments indicate some estimates of the standard deviations of β_T and β_e arising from assumed standard deviations of $\pm .01^\circ$ C and $\pm .015$ mb, respectively. Values occuring for $|T_{40} - T_{80}| < .04^\circ$ C or $|e_{40} - e_{80}| < .04$ mb are not plotted due to the excessively large errors to be expected under these conditions; here e refers to vapor pressure and the subscripts to the heights of measurement. The data do not indicate any significant difference between β_u and β_T, whereas β_e is unexpectedly small during lapse and near-adiabatic conditions.

It is shown by Lettau (1957) that the eddy diffusivities for momentum, heat and moisture must increase with height at different rates if the respective Deacon numbers differ. Therefore our over-water data suggest that the ratio of the eddy diffusivity for heat to that for momentum was roughly constant with height, whereas the ratio of the eddy diffusivity for vapor to that for momentum changed with height above the surface.

The near-isothermal temperature profiles, omitted in the above discussion, were accompanied by sea surface temperatures roughly 0.3° C warmer than the air. Similar apparent discrepancies, reported by Roll (1948) and by Deacon, *et al.* (1956), are noticeable in data published elsewhere. Roll's suggested explanation of evaporative cooling from the surface is incredible, because it implies a laminar water layer of some centimeters in depth. Deacon bases his explanation on Priestley's (1955) discussion of heat flux near the ground. The latter believes that above some level, near to but not coincident with the surface, an upward flux of heat can be maintained in an isothermal atmosphere; the mechanism responsible is supposedly free convection. Below that level the flux is maintained by "forced convection", that is, by mechanically driven eddies, and in this shallow layer a decrease of temperature with height must prevail. Our observations indicate that if such conditions did occur over the sea, the layer of forced convection lay below 40 cm.

Relative Profile Gradients. It is desirable to express the vertical gradient of a micrometeorological quantity in terms of a measurement at the surface and at a single height above. This requires introduction of a parameter which describes the relative profile gradient, such as the profile contour number (Lettau, 1957: 339) defined by

$$\alpha_q = z\frac{\partial q}{\partial z} \Big/ (q - q_0). \tag{6}$$

Again q is the property of the particular profile under consideration and q_0 its value at the surface. If α is regarded as a constant for a particular height above a water surface, the stress τ, for example, can then be written in terms of a single wind speed with the aid of (3) and (6), using $q = u$:

$$\sqrt{\tau/\varrho} = \frac{k\alpha_u}{1 - mz}\, u. \tag{7}$$

There have been numerous measurements of $k\alpha_u$ over water by a variety of methods. The most common of these, at low or moderate wind speeds, has been through use of (7), taking $k = 0.4$ but assuming $m = 0$ and using winds at two heights. In this case the product $k\alpha_u$, called the resistance coefficient, γ, by Sverdrup (1951),[3] is obtained from

$$k/\gamma = 1/\alpha_u = ln\, z/z_0 = ln\, z/z_2 + \frac{u_2}{u_1}\, ln\, z_2/z_1 \Big/ \left(\frac{u_2}{u_1} - 1\right) \qquad (8)$$

which follows from (3) and (7). From (8) it is evident that the resistance coefficient and contour number depend upon the reference height, z. It is also implicit in (8), but not so evident, that z_0 will have an apparent dependence upon stability due to the assumption of a logarithmic profile which may not actually exist. Therefore the resistance coefficient and profile contour numbers should be termed "apparent" when computed from (8), since they will also show an apparent variation with stability. Furthermore, it follows from (3) that the magnitude of this apparent variation will depend upon the heights of measurement, z_1, and z_2, under nonadiabatic conditions. Nevertheless it is of interest to present values of apparent contour number because they are directly comparable under adiabatic conditions to those found by other investigators if the same reference height is used. A height of 8 m will be used here in accordance with Sverdrup. In order to minimize the influence of the kinks in the wind profile, α_u was computed from winds at the four lowest levels by the method of least squares, assuming a logarithmic increase of wind speed with height. The values are shown in Fig. 4 (crosses) plotted against Richardson number at 80 cm. In the range of wind speeds encountered (3 to 9 m/sec) there did not appear to be any direct dependence of α_u on wind speed, that is, no dependence other than that introduced by the fact that wind speed and Richardson number are correlated. For convenience, a roughness length scale for z_0 is included on the left-hand side of Fig. 4. The adiabatic value for α_u is about 0.082, which is significantly smaller than the value 0.14 corresponding to the oft-quoted roughness length of 0.6 cm for the ocean (Sverdrup) and which is smaller than most of the values reported by Wagner (1958) for the Gulf of Mexico.

[3] Other writers have referred to γ^2 or $2\gamma^2$ as the resistance or friction coefficient.

Over water the profile contour numbers (eq. 6) for temperature and water vapor can also be measured if it is assumed that the temperature and vapor density of the air at the surface are the equilibrium values for sea water at the measured temperature. (The apparent profile contour number for water vapor, α_e, is frequently

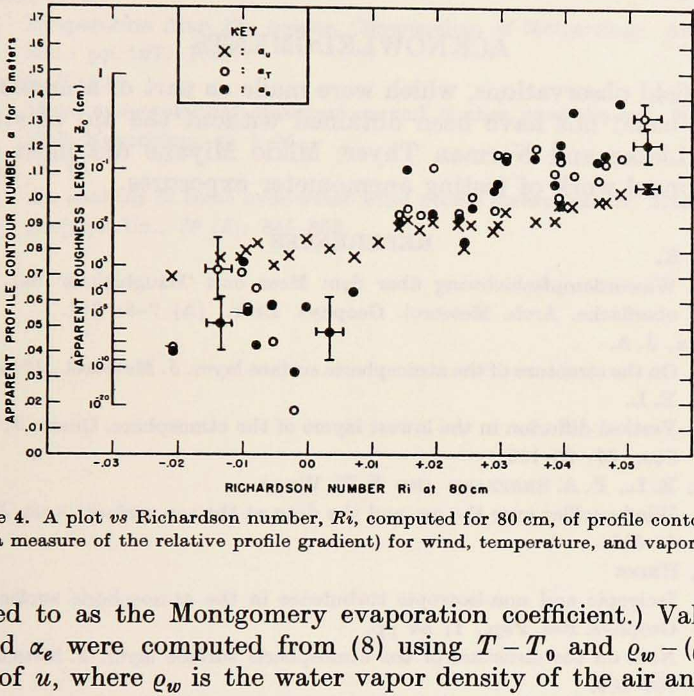

Figure 4. A plot *vs* Richardson number, *Ri*, computed for 80 cm, of profile contour number, α (a measure of the relative profile gradient) for wind, temperature, and vapor density.

referred to as the Montgomery evaporation coefficient.) Values of α_T and α_e were computed from (8) using $T - T_0$ and $\varrho_w - (\varrho_w)_0$ in place of u, where ϱ_w is the water vapor density of the air and $(\varrho_w)_0$ the saturation vapor density corrected for a salinity of 29 $^0/_{00}$. A height of 8 m was used for the reference level, and 40 and 160 cm for the levels of measurement. The profile contour numbers for temperature and water vapor are shown in Fig. 4 by open and solid circles, respectively. Four values of α_T have been omitted for periods when the air and sea surface temperatures were nearly equal. Within limits of observational error, α_T and α_e appear to be identical but show greater dependence upon Ri than does α_u. No significant secondary dependence of α_T or α_e upon wind speed was evident; this is in disagreement with Brocks (1955) who found such a dependence when he analyzed data gathered over the oceans by Wüst, Montgomery, and Sverdrup. Also, when his value of α_e for adiabatic temperature stratification and moderate wind speeds is adjusted to the same basis as those reported here, it is found to be 0.11, almost double the value of 0.06 which we found for similar conditions. On the other hand, our values of both α_u and α_e do agree closely with those which can be deduced from the data of Takahashi (1958) for Kagoshima Bay in southern Japan.

ACKNOWLEDGMENTS

The field observations, which were made as part of a meteorology course, could not have been obtained without the aid of students Bruce Lieske and Norman Thyer. Mikio Miyake did most of the wind-tunnel work of testing anemometer exposures.

REFERENCES

BROCKS, K.

1955. Wasserdampfschichtung über dem Meer und 'Raughigkeit' der Meeresoberflache. Arch. Meteorol. Geophys. Biok., (A) *7–8*: 354.

BUSINGER, J. A.

1955. On the structure of the atmospheric surface layer. J. Meteorol., *12*: 553–561.

DEACON, E. L.

1949. Vertical diffusion in the lowest layers of the atmosphere. Quart. J. R. met. Soc., *75*: 89–103.

DEACON, E. L., P. A. SHEPPARD AND E. K. WEBB

1956. Wind profiles over the sea and the drag at the sea surface. Aust. J. Phys., *9*: 511.

LETTAU, HEINZ

1949. Isotropic and non-isotropic turbulence in the atmospheric surface layer. Geophys. Res. Pap., 1; 84 pp.

1956. Note on the structure of the atmospheric surface layer. J. Meteorol., *13*: 507–509.

LETTAU, HEINZ AND BEN DAVIDSON

1957. Exploring the atmosphere's first mile. Pergamon Press, London, Vol. I.

MIDDLETON, W. E. K. AND A. F. SPILHAUS

1953. Meteorological instruments. Univ. of Toronto Press. 3rd ed. pp. 145–147.

MONIN, A. C. AND A. M. OBUKHOV

1953. Isotropic characteristics of turbulence in the atmospheric layer near the ground. Akad. Nauk SSSR, Doklady, *93* (2): 257–260.

PANOFSKY, H. A.

1952. A comparison of different types of stress measurement. Quart. J. R. met. Soc., *78*: 411–414.

PRIESTLEY, C. H. B.

1955. Free and forced convection in the atmosphere near the ground. Quart. J. R. met. Soc., *81*: 139–143.

ROLL, H. V.

1948. Über die vertikale Temperaturverteilung in der Wassernahen Luftschicht. Ann. Meteorol., *1*: 353–360.

SHEPPARD, P. A.

1958. Transfer across the earth's surface and through the air above. Quart. J. R. met. Soc., *84*: 205–224.

SVERDRUP, H. U.

1951. Evaporation from the oceans. Compendium of Meteorology. Amer. met. Soc.: pp. 1071–1081.

TAKAHASHI, TADAO

1958. Micro-meteorological observations and studies over the sea. Mem. Fac. Fish. Kagoshima, *6*: 1–46.

WAGNER, N. K.

1958. An analysis of some over-water wind profile measurements. Trans. Amer. geophys. Un., *39* (5): 845–852.

APPENDIX A

Hourly Period Number	*Date 1958*	*Local Time at Start of Period*	*WIND SPEED (cm/sec) at Listed Heights (cm)*							
			31	*60*	*91*	*133*	*171*	*213*	*291*	*442*
1	7/7	1530	613	672	685	728	733	764	789	837
2	7/7	1645	611	673	684	732	733	768	790	832
3*	7/7	1805	692	765	782	832	834	867	895	930
4†	7/7	1916	639	701	714	759	760	790	813	848
5	7/7	2142	665	706	746	772	807	807	848	883
6	7/8	0537	468	506	516	543	547	558	567	581
7	7/8	0705	424	464	468	498	494	513	518	535
8	7/8	0820	289	319	323	342	340	356	358	373
9	7/8	0933	317	345	354	373	375	393	402	427
10	7/8	1046	351	382	392	417	420	441	456	487
11	7/8	1202	338	369	378	403	406	429	444	481
12	7/8	1312	378	415	426	456	459	485	501	540
13	7/8	1426	374	408	420	448	452	475	493	530
14	7/8	1541	342	374	386	413	419	445	464	506
15	7/8	1647	345	378	391	419	424	450	470	507
16	7/8	1755	326	358	369	396	401	425	443	480
17	7/8	1910	273	301	313	339	343	365	379	406
18	7/9	0721	375	400	408	427	434	442	452	464
19	7/9	0830	382	408	417	438	444	456	464	474
20	7/9	0945	266	286	294	308	310	320	327	339
21	7/9	1059	206	225	228	240	241	251	258	270
22	7/9	1507	370	402	413	441	445	466	483	507
23	7/9	1615	368	405	418	450	457	471	506	547
24	7/9	1733	345	388	397	430	439	467	493	532
25	7/9	1837	400	442	452	485	495	519	547	587
26	7/9	1947	413	449	460	489	499	518	543	576
27	7/10	0603	454	500	503	533	529	551	557	571
28	7/10	0710	404	446	449	475	472	491	496	506
29	7/10	0838	336	366	372	390	389	400	409	419
30	7/10	0945	340	375	378	398	401	413	422	434

* Anemometer reading at 442 cm is for first half of period only, due to faulty counter operation last half.

† Anemometer reading at 442 cm is for last half of period only, due to faulty counter operation first half.

APPENDIX B

Period Number	Temperature (° C) at Listed Height (cm) sfc.	40	80	160	320	Vapor Pressure (millibars) at Listed Height (cm) sfc.	40	80	160	320
1*	16.80	19.66	19.91	20.18	20.53	—	—	—	—	—
2†	16.00	19.68	20.04	20.36	20.83	17.91	16.13	15.91	15.81	15.49
3	15.76	19.34	19.68	20.02	20.42	17.60	16.52	16.38	16.26	16.18
4	15.21	17.70	17.88	18.15	18.41	17.01	15.63	15.51	15.39	15.22
5††	13.98	—	—	—	—	15.72	—	—	—	—
6	14.61	13.48	13.40	13.34	13.27	16.37	14.21	14.10	13.90	13.75
7	14.49	13.67	13.67	13.64	13.61	16.24	14.61	14.58	14.53	14.44
8	14.19	13.92	13.92	13.92	13.93	15.93	14.37	14.33	14.22	14.13
9	14.06	14.74	14.81	14.90	15.01	15.79	14.50	14.37	14.26	14.08
10	14.26	15.51	15.63	15.76	15.96	16.01	14.60	14.48	14.32	14.09
11	14.50	15.65	15.76	15.93	16.17	16.25	14.64	14.48	14.28	14.03
12	14.26	15.97	16.19	16.39	16.71	16.01	14.69	14.51	14.36	14.13
13	14.50	16.17	16.38	16.61	16.89	16.25	14.92	14.76	14.59	14.36
14	14.76	16.62	16.84	17.07	17.50	16.53	15.20	15.02	14.84	14.54
15	14.72	17.09	17.37	17.66	18.10	16.48	15.06	14.88	14.68	14.41
16	14.56	16.84	17.09	17.34	17.75	16.31	14.92	14.77	14.58	14.34
17	14.73	16.40	16.62	16.92	17.34	16.49	15.35	15.22	15.05	14.84
18	15.28	13.27	13.19	13.14	13.06	17.09	14.53	14.43	14.37	14.22
19	14.04	13.50	13.49	13.46	13.42	15.77	14.58	14.53	14.46	14.36
20	14.16	14.16	14.17	14.19	14.20	15.90	14.78	14.73	14.66	14.54
21	14.46	14.58	14.61	14.65	14.68	16.22	15.36	15.30	15.23	15.13
22	15.10	17.00	17.18	17.44	17.80	16.89	15.69	15.56	15.43	15.23
23	15.21	18.18	18.44	18.78	19.34	17.01	15.68	15.51	15.33	15.12
24	15.10	18.29	18.60	19.07	19.87	16.89	15.78	15.58	15.40	15.16
25	14.97	17.92	18.19	18.59	19.20	16.76	15.86	15.71	15.56	15.40
26	14.63	16.53	16.68	16.91	17.35	16.39	15.46	15.36	15.26	15.11
27	14.24	13.15	13.13	13.04	12.96	15.98	14.70	14.69	14.61	14.55
28	14.09	13.05	13.00	12.95	12.87	15.81	14.57	14.52	14.45	14.34
29	14.13	13.43	13.39	13.34	13.31	15.86	14.68	14.63	14.58	14.49
30	14.46	14.35	14.35	14.38	14.40	16.22	15.15	15.16	15.07	14.97

* Vapor pressures are missing due to wet-thermocouple becoming partially dry.

† Vapor pressures represent only a 39 minute average, due to wet-thermocouple being partially dry part of period.

†† Measurements are missing because electrical generator was swamped by a large wave.